

# Trade-Offs in Improving Biofuel Tolerance Using Combinations of Efflux Pumps

William J. Turner and Mary J. Dunlop\*

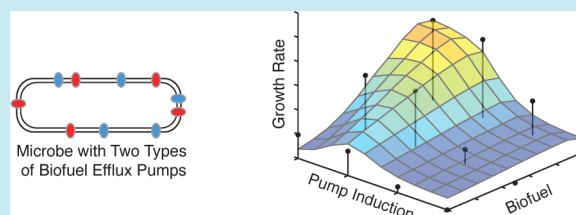
School of Engineering, University of Vermont, Burlington, Vermont 05405, United States

## S Supporting Information

**ABSTRACT:** Microbes can be engineered to produce next-generation biofuels; however, the accumulation of toxic biofuels can limit yields. Previous studies have shown that efflux pumps can increase biofuel tolerance and improve production. Here, we asked whether expressing multiple pumps in combination could further increase biofuel tolerance. Pump overexpression inhibits cell growth, suggesting a trade-off between biofuel and pump toxicity. With multiple pumps, it is unclear how the fitness landscape is impacted.

To address this, we measured tolerance of *Escherichia coli* to the biojet fuel precursor  $\alpha$ -pinene in one-pump and two-pump strains. To support our experiments, we developed a mathematical model describing toxicity due to biofuel and overexpression of pumps. We found that data from one-pump strains can accurately predict the performance of two-pump strains. This result suggests that it may be possible to dramatically reduce the number of experiments required for characterizing the effects of combined biofuel tolerance mechanisms.

**KEYWORDS:** biofuel tolerance, efflux pump, trade-off, cost-benefit, biofuel toxicity



Microbial production of next-generation biofuels has the potential to provide drop-in alternatives to liquid petroleum products including gasolines, diesels, and jet fuels.<sup>1</sup> Aviation fuels, in particular, represent an area where biofuels are especially important. In contrast to other transportation markets that have alternative renewable technologies (e.g., gasoline vs electric vehicles), aviation requires liquid fuels that are energy dense, work at low temperatures, and are not prohibitively expensive. Terpenes are naturally occurring compounds in plant biochemistry that have the potential to serve as next-generation jet fuels. Several studies have engineered pathways for terpene production in microbial hosts.<sup>2,3</sup> Recently, pinene has been synthesized as a jet fuel replacement.<sup>2–4</sup> Pinene dimers have a similar heating value and energy density to the tactical jet fuel JP-10 and can be readily synthesized from  $\alpha$ -pinene by chemical catalysis.<sup>2,5</sup>

Although they hold great promise as renewable jet fuels, end product inhibition is a critical factor in the microbial synthesis of monoterpenes.<sup>2,6</sup> Therefore, as biofuel production improves, it will be necessary to also improve host tolerance. As the intracellular concentration of biofuel increases, the protective barrier provided by the cell membrane is weakened and membrane permeability and fluidity increase from the breakdown of the tightly packed lipid bilayer. As a result, cellular machinery and energy can be released across the membrane in the form of ions, ATP, RNA, and proteins. This impacts electrochemical energy gradients such as the proton motive force that normally provide the driving force for essential transport processes.<sup>7,8</sup>

Microbes have evolved a wide variety of mechanisms to combat the effects of solvent toxicity.<sup>9,10</sup> These include

alteration in the membrane phospholipid composition for reduced permeability, active extrusion by efflux pumps, and heat shock protein assistance in the refolding of unraveled proteins.<sup>7,9</sup> Here, we focus on the transport of solvents by efflux pumps. Several previous studies have demonstrated that expression of pumps can improve biofuel production.<sup>11–13</sup> There is evidence that combinations of efflux pumps can confer additional tolerance compared to expression of individual pumps.<sup>14</sup> Notably, bacteria have evolved to have multiple parallel efflux pump systems. In *P. putida* DOT-T1E, toluene tolerance is achieved by three solvent resistant pumps, collectively known as the toluene tolerance genes (*ttg*), which work in concert to improve tolerance.<sup>15</sup> Here, we asked whether simultaneous heterologous expression of non-native efflux pumps in *E. coli* could enhance pinene tolerance relative to a wildtype control and strains containing individual pumps.

Overexpression of efflux pumps can be detrimental to growth, due to overloading of membrane insertion machinery and changes in membrane composition.<sup>9,16</sup> This creates a trade-off between pump toxicity and biofuel toxicity where moderate, but not high, expression is necessary to achieve optimal growth.<sup>17,18</sup> A similar trade-off has been observed with efflux pumps in antibiotic resistance.<sup>19</sup> With combinations of pumps, there are multiple sources of pump toxicity but also potential combinatorial benefits from reduced biofuel toxicity. Balancing these competing factors has the potential to introduce a complex fitness landscape. In addition, testing combinations of pumps under different induction conditions with different levels

Received: July 11, 2014

Published: December 12, 2014

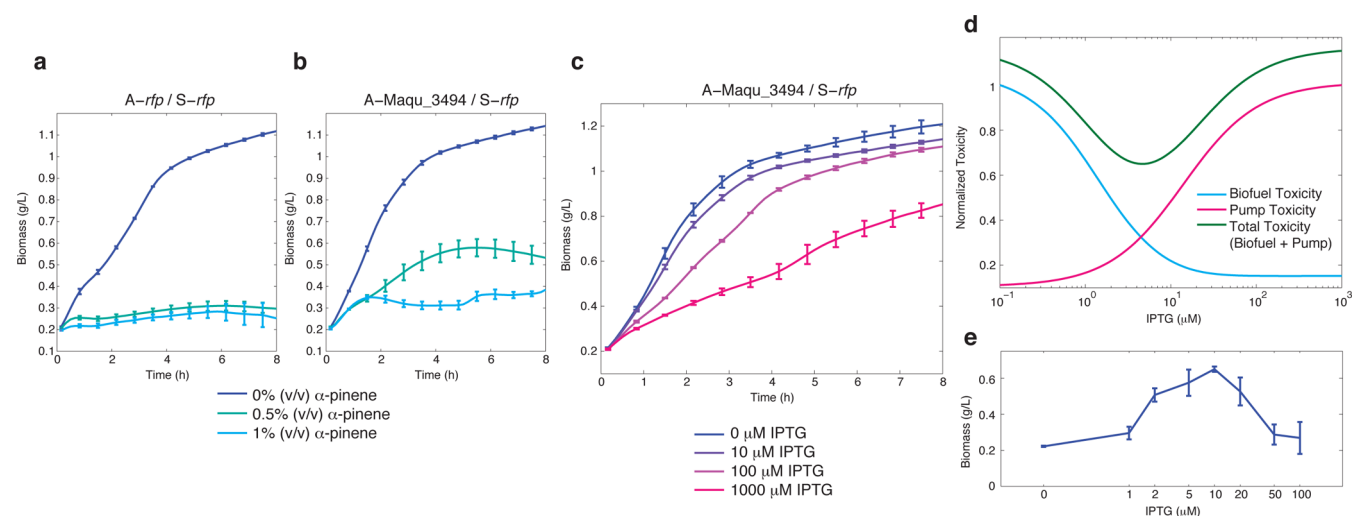


**Figure 1.** Costs and benefits of efflux pump expression. (a) The negative control, *E. coli* BW25113 with plasmids *A-rfp/S-rfp*, exhibits pinene toxicity. (b) Induction of a single pump strain *A-Maqu\_3494/S-rfp* with 10  $\mu\text{M}$  IPTG improves pinene tolerance. (c) Overexpression of Maqu\_3494 (strain *A-Maqu\_3494/S-rfp*) by IPTG induction inhibits growth. (d) Simulation results showing the cost and benefit of Maqu\_3494 expression in an environment containing 0.5% pinene. At low induction, biofuel toxicity is substantial, while at high induction pump toxicity dominates. The total toxicity is minimized at an intermediate level. Biofuel and pump toxicities are normalized by their maximum values. (e) Experimental data showing biomass after 8 h of growth with 0.5% pinene for the strain *A-Maqu\_3494/S-rfp* as a function of IPTG concentration. For a–c and e, error bars are the standard error of three biological replicates.

of biofuel quickly results in a large set of conditions requiring experimental characterization. Here, we show experimentally that a simple model of toxicities can help predict how two pumps act in concert, greatly reducing the number of validation experiments required.

In this study, we used four efflux pumps that are known to improve tolerance to  $\alpha$ -pinene.<sup>11</sup> Here, we refer to the pumps by the gene numbers of the inner membrane component; however, we note that each pump is composed of multiple genes (Methods). Pp\_3456 is native to *Pseudomonas putida* KT2440, Maqu\_3494, and Maqu\_0582 are from *Marinobacter aquaeolei*, and Abo\_0964 is from *Alcanivorax borkumensis* SK2. *P. putida* is a soil bacterium with known solvent tolerance properties,<sup>20</sup> *M. aquaeolei* is a hydrocarbon degrader that was isolated from the head of an offshore oil well,<sup>21,22</sup> and *A. borkumensis* is known to dominate hydrocarbon-rich marine environments like those near natural oil seepages or oil spills.<sup>23,24</sup> When tested individually in a strain of *E. coli* lacking the major native solvent-tolerance pump, all four pumps were shown to improve pinene tolerance.<sup>11</sup> In the present study, we comprehensively characterized the biofuel and pump toxicities for each pump individually and then combined pumps, repeating tolerance experiments. Using the single pump experimental data, we fit a mathematical model describing cell growth. From the single pump data we were able to predict the fitness landscape with multiple pumps using the mathematical model. This result captures the main features of all tested combinations of pump induction and biofuel levels. Importantly, this suggests that a small number of experiments may be sufficient to predict combinatorial effects between pumps.

## RESULTS AND DISCUSSION

In order to quantify the benefit of efflux pump expression and the toxicity of each pump, we performed growth assays with a gradient of pinene concentrations and different levels of pump induction (Methods). Because we were interested in testing

how combinations of pumps impacted growth, we used a two-plasmid system in all experiments. Using *E. coli* BW25113 as the host, we cotransformed cells with compatible medium copy (p15A origin) and low copy (SC101 origin) plasmids (Methods). As a negative control, we expressed red fluorescent protein (*rfp*) and compared this to expression of each efflux pump, individually or in combination. For concise notation, we refer to the medium copy plasmid (p15A) as “A” and the low copy plasmid (SC101) as “S.” For example, *A-rfp/S-rfp* is the negative control, expressing no non-native efflux pumps, and *A-Maqu\_3494/S-rfp* is a single pump strain, with Maqu\_3494 expressed from the medium copy plasmid.

In the wildtype strain, we observed a severe growth impact with 0.5% and 1% pinene (Figure 1a). Although the pinene levels tested here are well above those produced in engineered strains at present (e.g., 0.004%, or 32 mg/L in *E. coli*<sup>2</sup>), improving tolerance can increase yields even when the biofuels being produced are well below toxic levels.<sup>11</sup> We next expressed Maqu\_3494 under the control of the lacUV5 promoter (*A-Maqu\_3494/S-rfp*) and induced cultures with 10  $\mu\text{M}$  IPTG, resulting in low-to-moderate induction of the pump. The strain harboring the pump was able to partially restore growth in the presence of 0.5% and 1% pinene (Figure 1b). Next, we measured the impact of pump toxicity by adjusting the level of IPTG induction in the absence of pinene. Figure 1c shows the effect of Maqu\_3494 overexpression on growth. As the inducer concentration is increased, the cells grow more slowly. These data show the independent effects of biofuel and pump toxicity, suggesting a trade-off when optimizing efflux pump expression.

To interpret the toxicity trade-off, we used the experimental data from *A-Maqu\_3494/S-rfp* to fit a mathematical model describing cell growth, biofuel, and pump toxicity (Methods). The model is based on the Monod growth equation,<sup>25</sup> with modifications to account for biofuel and pump toxicity. We ran simulations for a range of inducer concentrations at a fixed pinene concentration and recorded the intracellular pinene and the final pump levels (Figure 1d). The combined impact of

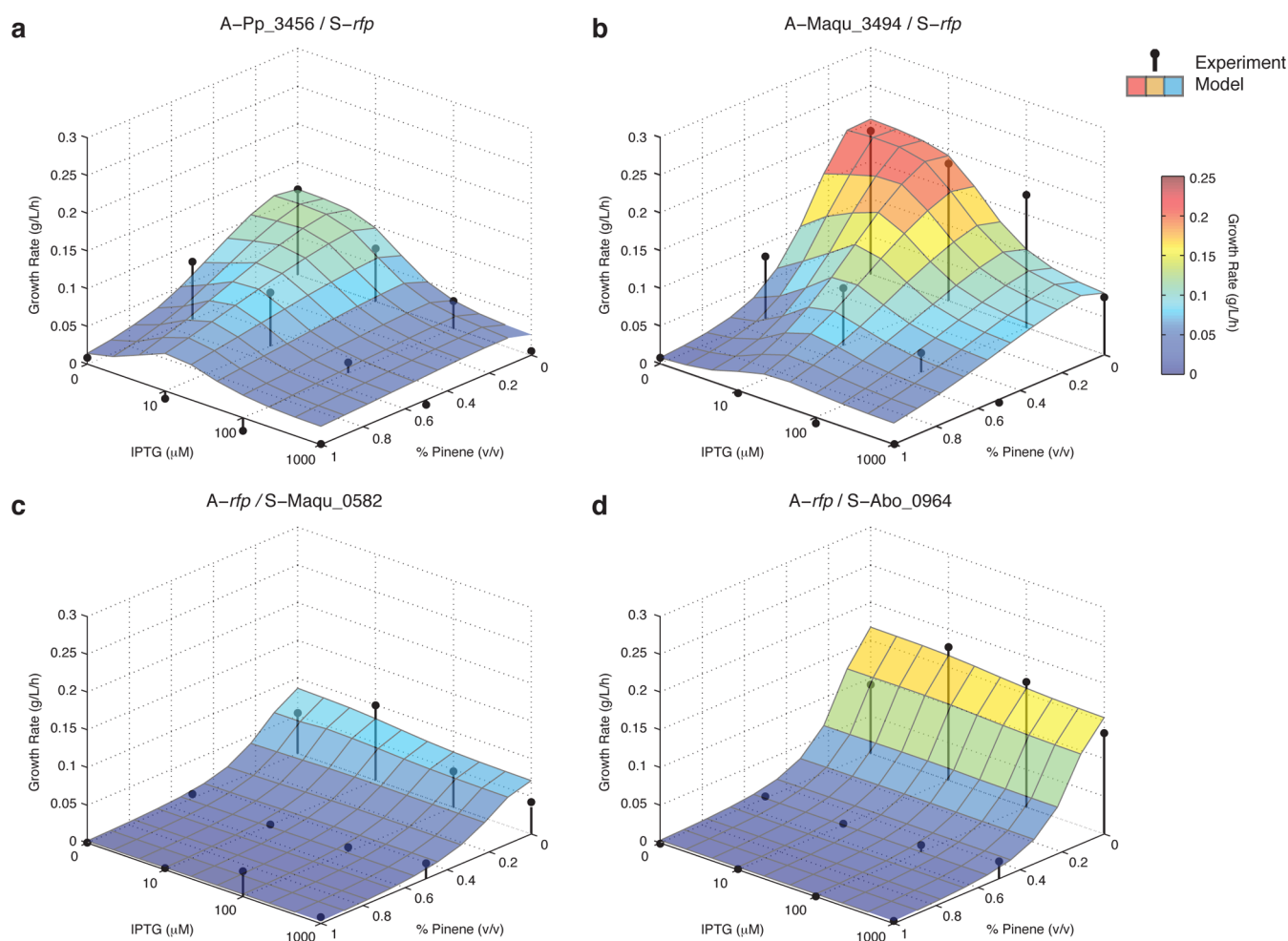


**Figure 2.** Fitness landscapes resulting from heterologous expression of single efflux pumps for a range of pinene and IPTG concentrations. Black dots represent the experimentally measured mean growth rate in exponential phase at each set of conditions. The colored surfaces show the same metric from simulated growth curves, as predicted by the mathematical model. Fitness landscapes are shown for four single-pump strains: (a) A-Pp\_3456/S-*rfp*, (b) A-Maqu\_3494/S-*rfp*, (c) A-*rfp*/S-Maqu\_0582, and (d) A-*rfp*/S-Abo\_0964. Error bars for the experimental data are shown in Supporting Information Figure S1a and error metrics are listed in Supporting Information Table S1.

biofuel and pump toxicity shows a clear minimum, suggesting that an intermediate induction level will maximize cell growth. We validated this experimentally by growing cells in the presence of 0.5% pinene with varying levels of IPTG induction (Figure 1e). As predicted by the model, growth in the presence of pinene is maximized at an intermediate induction level.

Next, we comprehensively characterized biofuel and pump toxicity for four efflux pumps. We chose three pinene and four IPTG concentrations ranging from zero to complete inhibition and induction respectively, for a total of 12 biofuel–inducer pairs. We performed growth assays using four single-pump strains: A-Pp\_3456/S-*rfp*, A-Maqu\_3494/S-*rfp*, A-*rfp*/S-Maqu\_0582, and A-*rfp*/S-Abo\_0964. In all cases, efflux pump expression is under control of the *lacUV5* promoter and induced by IPTG. Recall that 0.5% pinene completely inhibits growth in the wildtype strain. Thus, the experiments with Pp\_3456 and Maqu\_3494 show improvements in pinene tolerance at low and moderate levels of induction (Figure 2a, b). In addition, the effect of pump toxicity is visible in these strains, with higher levels of IPTG corresponding to a reduced growth rate. In contrast, the Maqu\_0582 and Abo\_0964 data show weak improvements in pinene tolerance, and although the pumps are toxic, as evidenced by a reduced growth rate in the

absence of pinene and IPTG, further induction does not have a dramatic effect on growth (Figure 2c, d). We selected these strains initially based on their improvement of pinene tolerance in a previous study;<sup>11</sup> however, differences between the strains and plasmids likely account for the reduced pump performance here. Overall, these experiments map the fitness landscapes for four individual efflux pumps under different biofuel and induction conditions, revealing trade-offs in pump expression and tolerance.

Given our data set on growth rates for biofuel and inducer pairs, we next asked whether our mathematical model could capture the fitness landscape trade-offs. Using the experimental data, we first modeled the impact of pinene toxicity (Methods). The parameters were determined using data from the wild type strain, A-*rfp*/S-*rfp*, and were then held constant across all subsequent simulations. Next, we used the data from each individual pump to fit the parameters associated with pump toxicity and biofuel export. The modeled fitness landscapes capture the features observed in the experimental data, including the interplay between biofuel and pump toxicities for the four distinct pumps (Figure 2). Our modeling results are significant because they indicate that it may be possible to measure only a subset of data points in a fitness landscape,

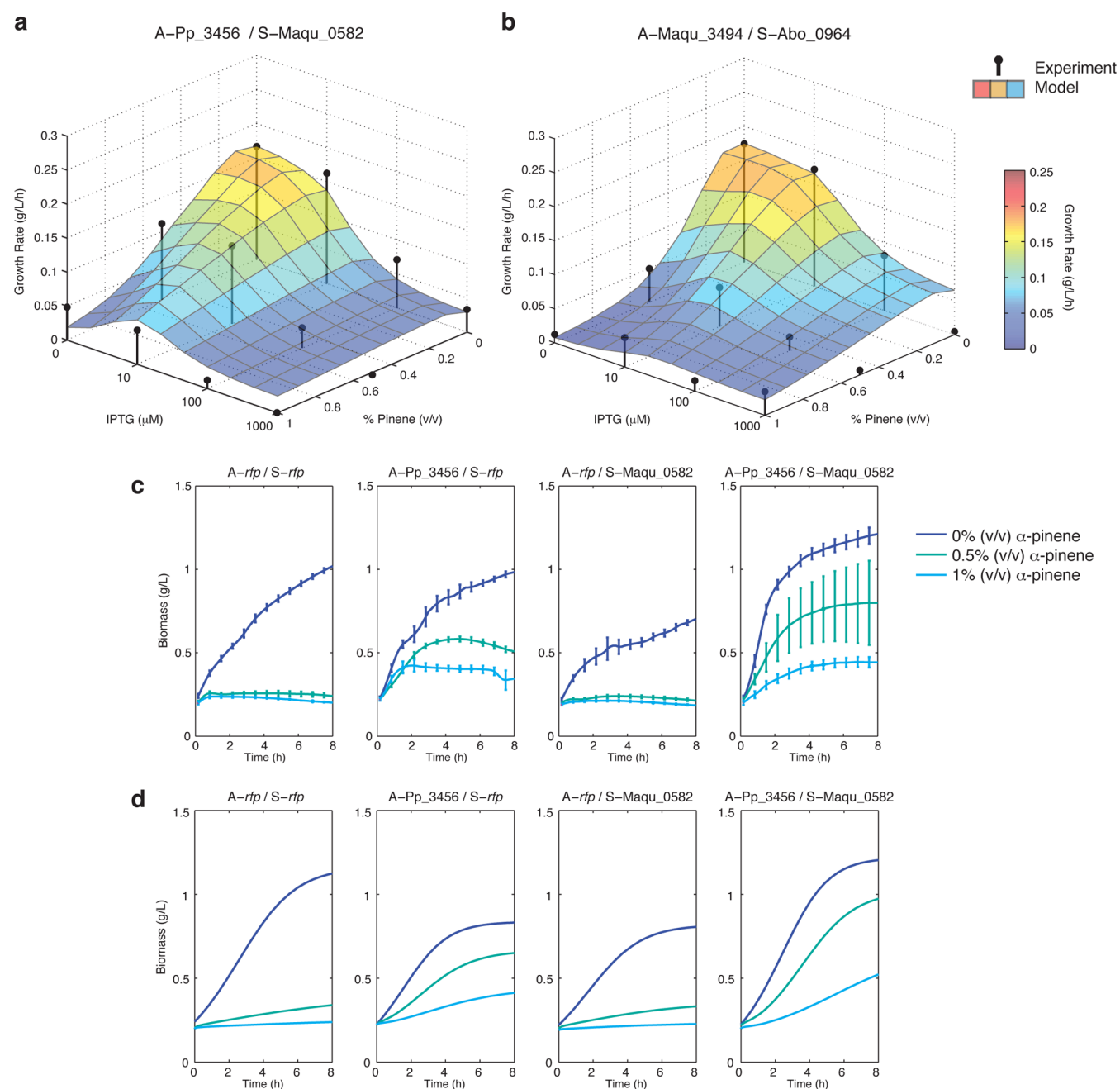


**Figure 3.** Fitness landscapes and growth curves resulting from simultaneous heterologous expression of two efflux pumps. Growth rate in exponential phase as a function of pinene and IPTG for strains with two pumps: (a) A-Pp\_3456/S-Maqu\_0582 and (b) A-Maqu\_3494/S-Abo\_0964. Black dots show experimental data; colored surface map is the modeling prediction. For error bars and analysis see Supporting Information Figure S1b, Table S1. (c) Experimental growth curves for no pump, single pump, and two pump strains with 0  $\mu$ M IPTG. Error bars show standard error for three replicates. (d) Mathematical modeling predictions for the same conditions as in c.

rather than exhaustively mapping all combinations. In addition, the model of individual pumps can be used to produce testable predictions about what happens when pumps are used in combination.

Using the pumps we characterized individually, we next constructed strains harboring two heterologously expressed efflux pumps. We tested A-Pp\_3456/S-Maqu\_0582 and A-Maqu\_3494/S-Abo\_0964 with different combinations of pinene and IPTG (Figure 3a, b). Although Maqu\_0582 acting alone showed little increase in pinene tolerance, the strain with both Pp\_3456 and Maqu\_0582 exhibited an increase in growth rate in the presence of pinene. This effect is especially

noticeable at the 1% pinene concentration, where the combination of pumps outperforms the single pump strains. These results suggest that combinations of pumps, even including those that show limited benefit when expressed individually, may be able to improve tolerance. In principle, pumps from different sources could work together as chimeras using, for example, inner membrane and periplasmic proteins from one pump and outer membrane proteins from another. Previous studies have shown examples of efflux pumps that can function in this modular fashion.<sup>11,26</sup>

Using the model with parameters determined from the single pump strain, we were able to capture the shape of the fitness



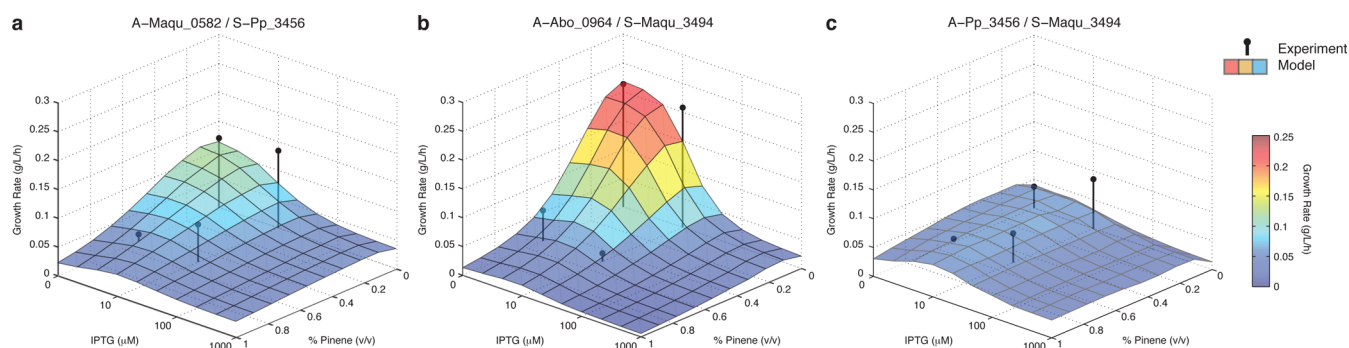


**Figure 4.** Experimental data and model predictions of fitness landscapes for additional pump combinations. (a) A-Maqu\_0582/S-Pp\_3456, (b) A-Abo\_0964/S-Maqu\_3494, and (c) A-Pp3456/S-Maqu\_3494. Black dots show experimental data for a subset of the pinene and IPTG conditions. The surface shows modeling predictions. Note that although the baseline growth rate for the A-Abo\_0964/S-Maqu\_3494 combination is higher, A-Maqu\_0582/S-Pp\_3456 and A-Pp3456/S-Maqu\_3494 both achieve a higher growth rate at 0.5% pinene, 10  $\mu$ M IPTG. The model predicts this trend to extend to higher biofuel and inducer concentrations. For error bars and analysis, see Supporting Information Figure S1c, Table S1.

landscape for both combinations of pumps (Figure 3a, b). To achieve this, we used the growth rate for the strain with no pinene or IPTG to set the relative position of the fitness landscape but otherwise changed no parameters (Methods). In other words, the parameters determined using the single pump strains, in combination with measurements from a single condition of the double pump strains, were sufficient to represent the entire fitness landscape for many different biofuel and pinene combinations.

In addition to the growth rate predictions, the model can also generate predictions of growth curve data. Here, we present data for the no pump, one pump, and two pump conditions for Pp\_3456 and Maqu\_0582, showing that the model captures the features of the experimental data (Figure 3c, d). Again, the modeling predictions from the two pump system are based on single pump measurements. Such a model-guided approach has the potential to drastically reduce the number of experimental measurements necessary to optimize biofuel tolerance.

We next asked whether the model could be used as a tool to predict the fitness landscape of a novel pump combination. To test this, we constructed A-Maqu\_0582/S-Pp\_3456, A-Abo\_0964/S-Maqu\_3494, and A-Pp\_3456/S-Maqu\_3494. We measured the baseline growth under 0% pinene and 0  $\mu$ M IPTG and then switched the pump expression rates to account for the plasmid copy number swap, leaving all other aspects of the model and its parameters unchanged. We then performed growth assays with a subset of the pinene and IPTG conditions (Figure 4a, b). Notably, both the model and the experimental data show the superior pinene tolerance of the A-Maqu\_0582/S-Pp\_3456 strain (Figure 4a) over the A-Abo\_0964/S-Maqu\_3494 strain (Figure 4b). This is visible in the experimental data at 0.5% pinene, where 10  $\mu$ M IPTG induction of the pumps leads to improved growth over the A-Abo\_0964/S-Maqu\_3494 strain. This is a nontrivial prediction, as the combined effects of the pumps without any pinene or IPTG would have suggested that this strain was inferior. We also tested A-Pp\_3456/S-Maqu\_3494. Individually, both pumps produced increases in pinene tolerance (Figure 2a, b). When combined, pump toxicity is substantial, though the strain retains improved pinene tolerance relative to the *A-rfp/S-rfp* control (Figure 4c).

This work provides a method for understanding trade-offs when using efflux pumps to improve biofuel tolerance of a host organism. By first testing single pump performance, selecting pumps that work well with the native biofuel tolerance

machinery, and then using the model to predict the performance of their combinations, it is possible to greatly reduce the number of experiments required to optimize the biofuel tolerance of a strain. Our model assumes that pump toxicity is multiplicative, which is a good approximation for the cases we tested; however, even in cases where this is not valid, the model can suggest a subset of experiments to perform. A limitation of our approach is that it is necessary to measure the performance of the strain at one condition (without pinene or IPTG) in order to set the baseline growth rate. We found that some pump combinations were highly toxic even with only basal pump expression (Figure 4c). In the future, improved models that capture synergistic or antagonistic effects in the absence of biofuel would be useful. For example, further experiments characterizing how heterologous pumps interact, and also, potential interactions with native *E. coli* efflux pumps such as AcrAB-TolC could further improve the model.

Optimization of pumps and their expression systems may further improve biofuel tolerance. For simplicity, we used a single inducer for both pumps, but in principle the pumps can be controlled independently. Further optimization using distinct inducible promoters is likely to match the best induction levels for each pump. Although we used inducible promoters for this work, several recent studies have demonstrated that biosensor-based feedback can improve growth by minimizing toxicity.<sup>27,28</sup> This approach can be combined with preliminary screens based on the methods presented here. In addition, the pumps used here have not been optimized for expression in *E. coli*; codon optimization, directed evolution, or other strategies could serve to further improve tolerance.<sup>12</sup> Further experimental data would also improve the model accuracy. For example, direct protein measurements of each of the components in the pump complexes could be used to measure the ratio of the two pumps and how their individual components interact. The ability to predict how combinations of tolerance mechanisms work together based on a small subset of experimental measurements has the potential to dramatically reduce the effort associated with engineering biofuel tolerance, leading to improved biofuel production strains.

## METHODS

**Bacterial Growth Conditions.** Cultures were grown in Luria Broth (LB) medium supplemented with 30  $\mu$ g/mL kanamycin and 35  $\mu$ g/mL chloramphenicol at 37C with 200 rpm orbital shaking. Overnight cultures were inoculated from a

single colony. Precultures were prepared by diluting overnight cultures 1:100 in selective LB medium and were grown for 2 h. Precultures were then diluted back to an optical density at 600 nm of approximately 0.2, IPTG was added to achieve concentrations of 0, 10, 100, or 1000  $\mu\text{M}$ , and the cultures were transferred to a 48-well plate (total volume per well of 500  $\mu\text{L}$ ).  $\alpha$ -pinene (Sigma) was added directly to the wells at concentrations of 0, 0.5, or 1% v/v. We note that pinene is insoluble in the growth medium and remains in a thin layer on the surface of the well. Plates were sealed with membranes to limit evaporation (Thermo Scientific AB-0580). Optical density readings and *rfp* fluorescence measurements (Supporting Information) were taken at 10 min intervals in a BioTek Synergy H1 plate reader. All experiments were performed in triplicate.

**Plasmids and Strains.** We used plasmid vectors pBbASk and pBbSSc from the BglBrick library.<sup>29</sup> The *rfp* plasmids from this library were used as controls. Efflux pumps were obtained from the library developed in ref 11. The pumps used here include all genes on the operon, which includes the inner membrane protein and periplasmic linker for Pp\_3456 and Maqu\_3494, and the inner membrane, periplasmic, and outer membrane proteins for Maqu\_0582 and Abo\_0964. The NCBI accession number for the inner membrane protein from Pp\_3456 is NP\_745594, Maqu\_3494 is YP\_960752, Maqu\_0582 is YP\_957870, and Abo\_0964 is YP\_692684. In the original library, the efflux pumps are on the pBbASk vector. To make pBbSSc variants, we amplified the efflux pump genes using PCR and cloned them into the pBbSSc vector, replacing *rfp* with the coding sequences associated with all pump components, as listed in ref 11. Plasmids were constructed using the Gibson assembly method.<sup>30</sup> pBbASk and pBbSSc plasmids were cotransformed into *E. coli* BW25113 and isolated on LB plates with kanamycin (30  $\mu\text{g}/\text{mL}$ ) and chloramphenicol (35  $\mu\text{g}/\text{mL}$ ).

**Growth Rate and Toxicity Calculations.** Optical density data at 600 nm from the plate reader experiments was converted to biomass (g/L) using an approximation of 1 g/L = 0.95 OD for exponential phase *E. coli*.<sup>31</sup> In order to eliminate single spurious data points to allow for derivative calculations, growth curves were preprocessed using a moving average filter with a window of five data points. In each window, the maximum and minimum of the subset were eliminated and the mean value of the remaining three points was calculated. Growth curve derivatives were calculated from the filtered data by taking the difference between the data points adjacent to each point and dividing by the two time intervals between them. The mean of the growth rate data in exponential phase, which we defined as 1–4 h, was used as the metric to assess the growth rate of the culture at each set of IPTG and pinene concentrations for both the experimental and simulated data (the sensitivity of the results to the selection of this time window is given in Supporting Information Table S2). Biofuel toxicity and pump toxicity (Figure 1d) were quantified as the intracellular biofuel or pump protein concentration after 100 h of simulation time. These values were normalized by the biofuel or pump protein concentration corresponding to complete inhibition.

**Mathematical Model.** A system of ordinary differential equations was used to model the rate of change of biomass  $N$ , growth substrate  $S$ , efflux pump on the medium copy plasmid  $P_1$  and low copy plasmid  $P_2$ , and intracellular pinene concentration  $C_i$ . Cell growth (eq 1) and substrate con-

sumption (eq 2) were modeled using a modified form of the Monod equation,<sup>25</sup> as in ref 32.

$$\dot{N} = \mu_{\max} N \frac{S}{K_s + S} \frac{1}{1 + \left(\frac{C_i}{K_c}\right)^h} \frac{1}{1 + \left(\frac{P_1}{K_{p1}}\right)^{h_{p1}}} \frac{1}{1 + \left(\frac{P_2}{K_{p2}}\right)^{h_{p2}}} \quad (1)$$

$$\dot{S} = -\frac{1}{\gamma} \mu_{\max} N \frac{S}{K_s + S} \quad (2)$$

For single pump strains, the maximum growth rate  $\mu_{\max}$ , growth yield  $\gamma$ , and half-saturation constant  $K_s$ , were adjusted to fit the toxicity profile specific to that pump (Supporting Information). The half-inhibition constant for pinene  $K_c$ , and the Hill coefficient  $h$ , were fit to the data for mean exponential growth rate as a function of pinene concentration for the wildtype strain, *A-rfp/S-rfp* from Figure 1a (Supporting Information Figure S2). The half-maximum inhibition constants for efflux pumps,  $K_{p1}$  and  $K_{p2}$ , and the corresponding Hill coefficients,  $h_{p1}$  and  $h_{p2}$ , were set to match the mean exponential growth rates of strains expressing the appropriate pump at the selected IPTG induction levels (Supporting Information Figure S3). For pump combinations, we set the baseline growth parameters  $\mu_{\max}$ ,  $\gamma$ , and  $K_s$  based on the growth observed in the absence of both pinene and IPTG; all other parameters are the same as those determined from the single pump experiments. Further details on model parameters and their selection are available in Supporting Information.

Pump expression (eqs 3 and 4) was modeled using the formula for chemically inducible expression from ref 17, with a maximum expression rate of  $\alpha_{p1/2}$  and threshold  $\gamma_1$ . These expression constants, along with basal expression rates  $\alpha_{p01/2}$  were attained from normalized *rfp* expression data for each of the plasmids (Supporting Information Figure S4).  $\beta$  is the pump protein degradation rate.

$$\dot{P}_1 = \alpha_{p01} + \alpha_{p1} \frac{I}{I + \gamma_1} - \beta P_1 \quad (3)$$

$$\dot{P}_2 = \alpha_{p02} + \alpha_{p2} \frac{I}{I + \gamma_1} - \beta P_2 \quad (4)$$

To model intracellular pinene concentration, a biofuel mass balance was incorporated to ensure that while mass could pass between the intracellular and extracellular domains, the total mass of pinene in the entire domain was constant. Passive diffusion of pinene through the cell membrane and export by efflux pumps was modeled by eq 5, as in ref 32, where  $C_i$  and  $C_e$  are the intra and extracellular pinene concentrations.

$$\dot{C}_i = \alpha_{c0} \frac{V_e}{V_i} (C_e - C_i) - C_i (\alpha_{c1} P_1 + \alpha_{c2} P_2) \quad (5)$$

The gradient of biofuel concentration across the cell membrane drives diffusion,<sup>33</sup> and the concentration change is accounted for by the ratio between the intracellular and extracellular volumes ( $V_i$  and  $V_e$ ) and the membrane permeability constant  $\alpha_{c0}$ . The rate of export of biofuel due to efflux pumps depends on the intracellular pinene concentration, the pump protein concentration, and the rate of export of each pump  $\alpha_{c1/2}$ , which were set to match experimental data for each individual pump. All model constants are listed in Supporting Information (Tables S3–

4). The sensitivity of the results to changes in the model parameters are shown in Supporting Information Figure S5.

Equation 1 uses the pump concentrations to improve growth through a reduction in toxicity. Note that higher pump levels do not necessarily correspond to improved growth. For instance, a pump might be toxic but not provide tolerance improvements.

All simulations were performed in MATLAB (MathWorks) using the ode23s solver.

## ■ ASSOCIATED CONTENT

### ● Supporting Information

Model constants and error analysis. This material is available free of charge via the Internet at <http://pubs.acs.org>.

## ■ AUTHOR INFORMATION

### Corresponding Author

\*mjdunlop@uvm.edu.

### Notes

The authors declare no competing financial interest.

## ■ ACKNOWLEDGMENTS

We thank the following individuals for their help with experiments and design: Yik Siu, Kristin Schutz, Aimee Shen, and all members of the Dunlop group. This work was supported by the Office of Science (BER) at the U.S. Department of Energy and the NASA Vermont Space Grant Consortium.

## ■ REFERENCES

- (1) Peralta-Yahya, P. P., Zhang, F., del Cardayre, S. B., and Keasling, J. D. (2012) Microbial engineering for the production of advanced biofuels. *Nature* 488, 320–328.
- (2) Sarria, S., Wong, B., Garcia Martin, H., Keasling, J. D., and Peralta-Yahya, P. (2014) Microbial synthesis of pinene. *ACS Synth. Biol.* 3, 466–475.
- (3) Yang, J., Nie, Q., Ren, M., Feng, H., Jiang, X., Zheng, Y., Liu, M., Zhang, H., and Xian, M. (2013) Metabolic engineering of *Escherichia coli* for the biosynthesis of  $\alpha$ -pinene. *Biotechnol. Biofuels* 6, 60.
- (4) Bokinsky, G., Peralta-Yahya, P. P., George, A., Holmes, B. M., Steen, E. J., Dietrich, J., Lee, T. S., Tullman-Ercek, D., Voigt, C. A., Simmons, B. A., and Keasling, J. D. (2011) Synthesis of three advanced biofuels from ionic liquid-pretreated switchgrass using engineered *Escherichia coli*. *Proc. Natl. Acad. Sci. U.S.A.* 108, 19949–19954.
- (5) Harvey, B. G., Wright, M. E., and Quintana, R. L. (2010) High-density renewable fuels based on the selective dimerization of pinenes. *Energy Fuels* 24, 267–273.
- (6) Brennan, T. C., Turner, C. D., Kromer, J. O., and Nielsen, L. K. (2012) Alleviating monoterpene toxicity using a two-phase extractive fermentation for the bioproduction of jet fuel mixtures in *Saccharomyces cerevisiae*. *Biotechnol. Bioeng.* 109, 2513–2522.
- (7) Dunlop, M. J. (2011) Engineering microbes for tolerance to next-generation biofuels. *Biotechnol. Biofuels* 4, 32.
- (8) Segura, A., Molina, L., Fillet, S., Krell, T., Bernal, P., Munoz-Rojas, J., and Ramos, J. L. (2012) Solvent tolerance in Gram-negative bacteria. *Curr. Opin. Biotechnol.* 23, 415–421.
- (9) Nicolaou, S. A., Gaida, S. M., and Papoutsakis, E. T. (2010) A comparative view of metabolite and substrate stress and tolerance in microbial bioprocessing: From biofuels and chemicals, to biocatalysis and bioremediation. *Metab. Eng.* 12, 307–331.
- (10) Ramos, J. L., Duque, E., Gallegos, M. T., Godoy, P., Ramos-Gonzalez, M. I., Rojas, A., Teran, W., and Segura, A. (2002) Mechanisms of solvent tolerance in gram-negative bacteria. *Annu. Rev. Microbiol.* 56, 743–768.

- (11) Dunlop, M. J., Dossani, Z. Y., Szmids, H. L., Chu, H. C., Lee, T. S., Keasling, J. D., Hadi, M. Z., and Mukhopadhyay, A. (2011) Engineering microbial biofuel tolerance and export using efflux pumps. *Mol. Syst. Biol.* 7, 487.

- (12) Fisher, M. A., Boyarskiy, S., Yamada, M. R., Kong, N., Bauer, S., and Tullman-Ercek, D. (2014) Enhancing tolerance to short-chain alcohols by engineering the *Escherichia coli* AcrB efflux pump to secrete the non-native substrate *n*-butanol. *ACS Synth. Biol.* 3, 30–40.

- (13) Teixeira, M. C., Godinho, C. P., Cabrito, T. R., Mira, N. P., and Sa-Correia, I. (2012) Increased expression of the yeast multidrug resistance ABC transporter Pdr18 leads to increased ethanol tolerance and ethanol production in high gravity alcoholic fermentation. *Microb. Cell Fact.* 11, 98.

- (14) Lee, A., Mao, W. M., Warren, M. S., Mistry, A., Hoshino, K., Okumura, R., Ishida, H., and Lomovskaya, O. (2000) Interplay between efflux pumps may provide either additive or multiplicative effects on drug resistance. *J. Bacteriol.* 182, 3142–3150.

- (15) Rojas, A., Duque, E., Mosqueda, G., Golden, G., Hurtado, A., Ramos, J. L., and Segura, A. (2001) Three efflux pumps are required to provide efflux tolerance to toluene in *Pseudomonas putida* DOT-T1E. *J. Bacteriol.* 183, 3967–3973.

- (16) Wagner, S., Baars, L., Ytterberg, A. J., Klussmeier, A., Wagner, C. S., Nord, O., Nygren, P. A., van Wijk, K. J., and de Gier, J. W. (2007) Consequences of membrane protein overexpression in *Escherichia coli*. *Mol. Cell Proteomics* 6, 1527–1550.

- (17) Dunlop, M. J., Keasling, J. D., and Mukhopadhyay, A. (2010) A model for improving microbial biofuel production using a synthetic feedback loop. *Syst. Synth Biol.* 4, 95–104.

- (18) Harrison, M. E., and Dunlop, M. J. (2012) Synthetic feedback loop model for increasing microbial biofuel production using a biosensor. *Front. Microbiol.* 3, 360.

- (19) Wood, K. B., and Cluzel, P. (2012) Trade-offs between drug toxicity and benefit in the multi-antibiotic resistance system underlie optimal growth of *E. coli*. *BMC Syst. Biol.* 6, 48.

- (20) Nelson, K. E., Weinel, C., Paulsen, I. T., Dodson, R. J., Hilbert, H., Martins dos Santos, V. A., Fouts, D. E., Gill, S. R., Pop, M., Holmes, M., Brinkac, L., Beanan, M., DeBoy, R. T., Daugherty, S., Kolonay, J., Madupu, R., Nelson, W., White, O., Peterson, J., Khouri, H., Hance, I., Chris Lee, P., Holtzapple, E., Scanlan, D., Tran, K., Moazzez, A., Utterback, T., Rizzo, M., Lee, K., Kosack, D., Moestl, D., Wedler, H., Lauber, J., Stjepandic, D., Hoheisel, J., Straetz, M., Heim, S., Kiewitz, C., Eisen, J. A., Timmis, K. N., Dusterhoft, A., Tumbler, B., and Fraser, C. M. (2002) Complete genome sequence and comparative analysis of the metabolically versatile *Pseudomonas putida* KT2440. *Environ. Microbiol.* 4, 799–808.

- (21) Huu, N. B., Denner, E. B., Ha, D. T., Wanner, G., and Stan-Lotter, H. (1999) *Marinobacter aquaeolei* sp. nov., a halophilic bacterium isolated from a Vietnamese oil-producing well. *Int. J. Syst. Bacteriol.* 49 (Pt 2), 367–375.

- (22) Singer, E., Webb, E. A., Nelson, W. C., Heidelberg, J. F., Ivanova, N., Pati, A., and Edwards, K. J. (2011) Genomic potential of *Marinobacter aquaeolei*, a biogeochemical “opportunist”. *Appl. Environ. Microbiol.* 77, 2763–2771.

- (23) Schneiker, S., Martins dos Santos, V. A., Bartels, D., Bekel, T., Brecht, M., Buhmester, J., Chernikova, T. N., Denaro, R., Ferrer, M., Gertler, C., Goesmann, A., Golyshina, O. V., Kaminski, F., Khachane, A. N., Lang, S., Linke, B., McHardy, A. C., Meyer, F., Nechitaylo, T., Puhler, A., Regenhardt, D., Rupp, O., Sabirova, J. S., Selbitschka, W., Yakimov, M. M., Timmis, K. N., Vorholter, F. J., Weidner, S., Kaiser, O., and Golyshin, P. N. (2006) Genome sequence of the ubiquitous hydrocarbon-degrading marine bacterium *Alcanivorax borkumensis*. *Nat. Biotechnol.* 24, 997–1004.

- (24) Yakimov, M. M., Golyshin, P. N., Lang, S., Moore, E. R. B., Abraham, W.-r., Lunsdorf, H., and Timmis, K. N. (1972) *Alcanivorax borkumensis* gen. nov., sp. nov., a new, hydrocarbon-degrading and surfactant-producing marine bacterium. *Int. J. Syst. Bacteriol.* 48, 339–348.

- (25) Monod, J. (1949) The growth of bacterial cultures. *Annu. Rev. Microbiol.* 3, 371–394.

(26) Elkins, C. A., and Nikaido, H. (2002) Substrate specificity of the RND-type multidrug efflux pumps AcrB and AcrD of *Escherichia coli* is determined predominately by two large periplasmic loops. *J. Bacteriol.* 184, 6490–6498.

(27) Dahl, M. K., Msadek, T., Kunst, F., and Rapoport, G. (1992) The phosphorylation state of the degu response regulator acts as a molecular switch allowing either degradative enzyme-synthesis or expression of genetic competence in *Bacillus subtilis*. *J. Biol. Chem.* 267, 14509–14514.

(28) Zhang, F., Carothers, J. M., and Keasling, J. D. (2012) Design of a dynamic sensor-regulator system for production of chemicals and fuels derived from fatty acids. *Nat. Biotechnol.* 30, 354–359.

(29) Lee, T. S., Krupa, R. A., Zhang, F., Hajimorad, M., Holtz, W. J., Prasad, N., Lee, S. K., and Keasling, J. D. (2011) BglBrick vectors and datasheets: A synthetic biology platform for gene expression. *J. Biol. Eng.* 5, 12.

(30) Gibson, D. G., Young, L., Chuang, R. Y., Venter, J. C., Hutchison, C. A., 3rd, and Smith, H. O. (2009) Enzymatic assembly of DNA molecules up to several hundred kilobases. *Nat. Methods* 6, 343–345.

(31) Neidhardt, F. (1996) *Escherichia coli and Salmonella: Cellular and Molecular Biology*, ASM Press, Washington, DC.

(32) Frederix, M., Hutter, K., Leu, J., Batth, T. S., Turner, W. J., Ruegg, T. L., Blanch, H. W., Simmons, B. A., Adams, P. D., Keasling, J. D., Thelen, M. P., Dunlop, M. J., Petzold, C. J., and Mukhopadhyay, A. (2014) Development of a native *Escherichia coli* induction system for ionic liquid tolerance. *PLoS One* 9, e101115.

(33) Deris, J. B., Kim, M., Zhang, Z., Okano, H., Hermsen, R., Groisman, A., and Hwa, T. (2013) The innate growth bistability and fitness landscapes of antibiotic-resistant bacteria. *Science* 342, 1237435.